

Tuning magnetic properties by roll-up of Au/Co/Au films into microtubes

C. Müller, M. S. Khatri, C. Deneke, S. Fähler, Y. F. Mei, E. Bermúdez Ureña, and O. G. Schmidt

Citation: *Appl. Phys. Lett.* **94**, 102510 (2009); doi: 10.1063/1.3095831

View online: <https://doi.org/10.1063/1.3095831>

View Table of Contents: <http://aip.scitation.org/toc/apl/94/10>

Published by the [American Institute of Physics](#)

Articles you may be interested in

[Towards compact three-dimensional magnetoelectronics—Magnetoresistance in rolled-up Co/Cu nanomembranes](#)

Applied Physics Letters **100**, 022409 (2012); 10.1063/1.3676269

[Optical properties of rolled-up tubular microcavities from shaped nanomembranes](#)

Applied Physics Letters **94**, 141901 (2009); 10.1063/1.3111813

[Exceptional transport property in a rolled-up germanium tube](#)

Applied Physics Letters **110**, 112104 (2017); 10.1063/1.4978692

[Rolled-up micro- and nanotubes from single-material thin films](#)

Applied Physics Letters **89**, 223109 (2006); 10.1063/1.2390647

[Uniaxial and tensile strained germanium nanomembranes in rolled-up geometry by polarized Raman scattering spectroscopy](#)

AIP Advances **5**, 037115 (2015); 10.1063/1.4914916

[High-performance giant magnetoresistive sensorics on flexible Si membranes](#)

Applied Physics Letters **106**, 153501 (2015); 10.1063/1.4918652



5 Electronic Measurement Pitfalls to Avoid

Get the whitepaper

Tuning magnetic properties by roll-up of Au/Co/Au films into microtubes

C. Müller,^{1,a)} M. S. Khatri,² C. Deneke,¹ S. Fähler,² Y. F. Mei,¹ E. Bermúdez Ureña,¹ and O. G. Schmidt¹

¹Institute for Integrative Nanosciences, IFW Dresden, Helmholtzstraße 20, D-01069 Dresden, Germany

²Institute for Metallic Materials, IFW Dresden, Helmholtzstraße 20, D-01069 Dresden, Germany

(Received 25 November 2008; accepted 16 February 2009; published online 11 March 2009)

Au/Co/Au trilayers are fabricated by tilted deposition on prestructured polymer sacrificial layers. The metal trilayers are released by selectively dissolving the sacrificial layer and roll-up into microtubes. Magnetization properties are strongly affected by the roll-up process. In addition to a modified shape anisotropy, the magnetostrictive anisotropy due to the anisotropic stress release is reversed. Low temperature measurements support the presence of significant exchange bias in these rolled-up structures. © 2009 American Institute of Physics. [DOI: 10.1063/1.3095831]

Generally, the magnetic properties of small ferromagnetic elements are governed by their size and shape in addition to their intrinsic material parameters. Various shapes such as squares,¹ rings,² wires,³ and tubes^{4,5} have been reported. Among them, ring-shaped and tubular structures are of much interest due to a low influence of edge roughness and their minimal stray field, resulting in uniform and reproducible switching characteristics. In particular, tubular structures with a low density, which can float in fluids, and with a large surface available for functionalization are promising candidates for *in vivo* applications (e.g., particle targeting and molecule separation).⁶

Strain engineering has been used to prepare rolled-up micro- and nanotubes based on semiconductor materials in the past years.^{7,8} More recently, a method to rearrange prestressed nanomembranes into micro- or nanotubes on polymers has extended the range of material systems, including magnetic materials.⁶ This technique allows the fabrication of individual tubes as well as large tube arrays in a controlled way. The magnetic tubes created in this fashion have been employed as remotely controlled microjet engines^{6,9} and magnetofluidic sensors.¹⁰ However, to date, no systematic investigations of the roll-up process on the magnetic properties of such tubes have been reported.

In this letter, nanocrystalline microtubes are prepared by the roll-up of the corresponding Au/Co/Au layer stack. The tube diameter is shown to be scalable with the metal film thickness, while their lengths are predefined by the lithographically adjusted pattern size. Structural and chemical analyses reveal that the walls of the microtubes consist of a periodic layer structure. A comparison of the magnetization behavior along the key directions of the prestressed layer stack and the microtubes is used to understand the origin of magnetic anisotropy. Additionally, the effect of the temperature on the magnetization reversal and exchange bias (EB) is studied.

To fabricate the rolled-up microtubes, photoresist layers (ARP-3510 positive resist) with a thickness of $\sim 2 \mu\text{m}$ on Si (001) were patterned into well-defined squares (20×20 , 50×50 , and $100 \times 100 \mu\text{m}^2$) by utilizing conventional photolithography. Thin Au(4 nm)/Co(x)/Au(4 nm) layers were deposited by electron beam deposition at a pressure of $< 10^{-4}$ Pa onto the photoresist layer. A Co film thickness x

between 7 and 22 nm was used. The tilted deposition was performed with an angle of 61° in relation to the normal incidence of the material flux. Using this technique, one side of the photoresist edge becomes shadowed, which facilitates a rolling up of the film in a predefined direction.¹¹ Subsequently, the Au/Co/Au films were rolled-up by dissolving the photoresist layer with acetone. In order to avoid deformation or collapse of the structures, the organic solvent was removed afterward using a supercritical drying step.

Morphology and size of the microstructures were examined using optical microscopy and scanning electron microscopy (SEM). A cross-section of a microtube was carefully prepared by focused ion beam etching using a Zeiss NVision. The obtained lamella was investigated with transmission electron microscopy (TEM) in a FEI Tecnai T20 at 200 kV equipped with an energy dispersive x-ray (EDX) detector for chemical analysis. Magnetic measurements of the planar film and ordered microtube arrays in all key directions were performed in a Quantum Design physical properties measurement system equipped with a vibrating sample magnetometer (VSM) and magnetic field applied in either the parallel or perpendicular direction to the sample. In addition, hysteresis loops of individual film patterns and tubes were measured using a NANOMOKE magnetometer in which the probing laser was focused to $\sim 3 \mu\text{m}$.

Figure 1(a) shows an optical microscopy image of well-aligned Au/Co/Au microtubes. Each of them was obtained from a $100 \times 100 \mu\text{m}^2$ large film square. After releasing the prestressed layers, the fraction of microtubes amounts to 90% of the magnetic material, whereas the rest of 10% originates from the Au/Co/Au film located in between the rolled areas [bright stripes in Fig. 1(a)]. A SEM image of a typical single microtube with a diameter of $\sim 5 \mu\text{m}$ and a sketch of the rolling process are illustrated in Fig. 1(b). The driving force for roll-up is the relaxation of stress gradients across the metallic layer stack depending on the deposition parameters (growth rate and substrate temperature).⁶ In Fig. 1(c) the scalability of the tube diameter¹² as a function of total layer thickness is summarized. All the samples were grown at room temperature and with growth rates of ~ 0.05 and ~ 0.15 nm/s for the Au and the Co layers, respectively. A variation in the metal layer thickness allows us to tune the tube diameter between ~ 2 and $\sim 11 \mu\text{m}$, corresponding from one to ten windings. An additional control parameter is the area of the pattern, and smaller areas result in smaller tube diameters. The latter effect is believed to originate from

^{a)}Electronic mail: christian.mueller@ifw-dresden.de.

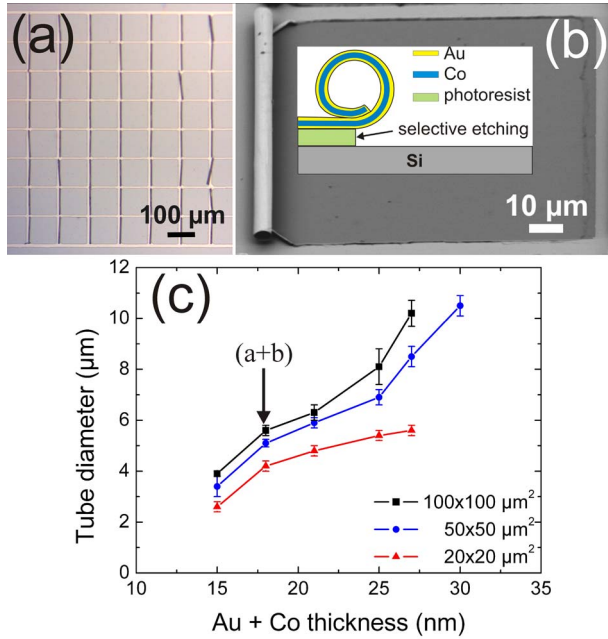


FIG. 1. (Color online) (a) Optical microscopy image of a periodic microtube array obtained after roll-up of 4 nm Au/10 nm Co/4 nm Au trilayers. (b) SEM image of a microtube with a diameter of roughly 5 μm . The inset schematically describes the roll-up process. (c) Plot of tube diameter as a function of total thickness and pattern size for a series of Au/Co/Au samples with similar deposition parameters. (a+b) marks the analyzed sample.

a dependency of the stress relaxation mechanism along two different directions (tube axis and roll-up direction) during the roll-up process.¹³

Figure 2 summarizes the cross-sectional microscopic structure of the tubes. The periodic arrangement of the Au/Co/Au layers is shown in Fig. 2(a). A ~ 3 nm thick gap between adjacent windings, accompanied by a significant surface roughness, is visible. The different materials can be distinguished by their material contrast [Fig. 2(b)], which enables us to estimate a thickness for the Au layer of ~ 3 nm and for the Co layer of ~ 12 nm, in agreement with the

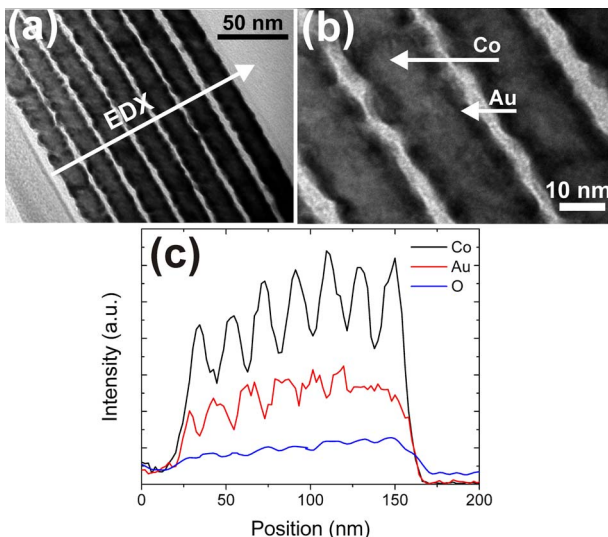


FIG. 2. (Color online) (a) TEM cross-section image of a rolled-up microtube from 4 nm Au/10 nm Co/4 nm Au trilayers. (b) HRTEM image from the tube walls also indicating the regions for Co and Au. (c) Corresponding EDX line scans for Co, Au, and O after scanning along the marked line in (a).

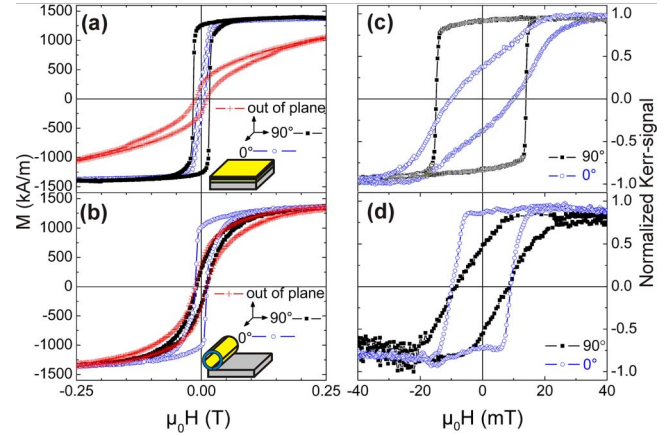


FIG. 3. (Color online) VSM hysteresis loops of (a) a 4 nm Au/10 nm Co/4 nm Au film array and (b) the corresponding tube array after the roll-up process at 300 K. The insets show the directions of the applied magnetic field. MOKE hysteresis loops measured along both in-plane directions (c) on a single film pattern and (d) on a single tube.

nominal deposition parameters. Furthermore, the EDX mapping recorded along the direction marked in Fig. 2(a) verifies the elemental distribution. EDX line scans for Co, Au, and O are displayed in Fig. 2(c), and seven periods of the Au/Co/Au layer sequence can be clearly identified.

In Fig. 3 we present typical magnetization curves for the Au/Co/Au films and the corresponding rolled-up tubes measured at 300 K. These measurements were performed with the same samples used for the structural investigations. Measurements of the film [Fig. 3(a)] perpendicular to the substrate surface reveal a hard axis loop with low slope and low coercivity H_c of 12 mT, as expected due to shape anisotropy. The saturation magnetization M_S for the film is close to the value for bulk Co (1.4×10^6 A/m). Unexpectedly, we observe a pronounced difference when measuring hysteresis loops for different directions within the film plane. Measurements along 90° (the direction of inclined deposition) exhibit a typical easy axis rectangular loop with H_c of 17 mT. The coercivity along 0° is smaller (~ 10 mT), and the curve is significantly more tilted. The intersection of both in-plane curves gives an average anisotropy field of $H_A = 2K/M_S$ of 12 mT, which is equal to an anisotropy constant of $K = 8 \times 10^3$ J/m³. The absence of hcp-Co reflections within XRD measurements (not shown) as well as the absence of any pronounced microstructure in the TEM images allows us to attribute this anisotropy entirely due to stress. The difference of stress along both in-plane directions can be estimated from

$$K = 3/2\lambda_S\sigma, \quad (1)$$

where λ_S is the magnetostrictive constant and σ is the stress.¹⁴ Using the value for Co $\lambda_S = -62 \times 10^{-6}$ (Ref. 15) one obtains a difference of stress between both in-plane directions of ~ 86 MPa. The sign suggests a more compressive stress along 90° compared to the 0° direction ($\sigma_{0^\circ} - \sigma_{90^\circ} < 0$). As a conclusion, the orientation of the easy axis seems to be supported by this external uniaxial stress, which was induced during the deposition process.

After roll-up the magnetization behavior changes completely [Fig. 3(b)]. First, the magnetic in-plane anisotropy is reversed, and the magnetic saturation field along the out-of-plane direction is significantly decreased. The observed

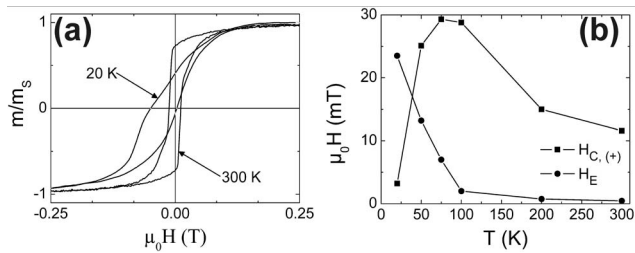


FIG. 4. (a) FC hysteresis loops at 20 and 300 K. (b) Temperature dependence of the coercive field $H_{c(+)}$ and of the EB field H_E of a Au/Co/Au microtube array after FC (+0.5 T). The field was applied along the tube axis.

curve shape suggests that shape anisotropy tries to locally align the magnetization within the tube surface, but the integral VSM measurements average over all directions of the local surface with the direction of the applied field. Second, since stress release only occurred along 90° ($\sigma_{90^\circ}=0$), just the lower compressive stress along 0° ($\sigma_{0^\circ}<0$) remains. Hence, the easy axis of magnetization is now aligned along 0° . In comparison to the film, H_c along the easy axis is smaller and amounts to 13 mT. For tubes with an ideal cylindrical cross-section the directions normal to the tube axis are expected to be equal. In fact, identical values for H_c of 11 mT are obtained, but small differences in the slope of the hysteresis are observed. These small differences may originate from deviations of the ideal cylindrical structure. As already described in the beginning, a small continuous film contribution is superimposed in these hysteresis loops. However, these individual contributions can be well separated by magneto-optical Kerr effect (MOKE) investigations using the longitudinal MOKE. Measurements on individual prestressed film patterns in Fig. 3(c) and single rolled-up tubes in Fig. 3(d) clearly exhibit the evolution of magnetic anisotropy. These measurements confirm the conversion of easy and hard in-plane magnetization axes within the film plane by roll-up. Since the values for H_c from this individual tube are in good agreement with the VSM measurements, these findings prove the high perfection of the arrays and show that the small contributions of the continuous film do not affect the switching behavior of the tube array.

In addition to the measurements at room temperature, hysteresis of the tube array after field cooling (FC, +0.5 T, along the tube axis) was measured at low temperatures. The shifted hysteresis, exemplarily shown for 20 K [Fig. 4(a)] suggests a pronounced negative EB effect due to the exchange coupling at ferromagnetic/antiferromagnetic interfaces.¹⁶ The presence of small amounts of O within the samples [Fig. 2(c)] can be an indication that some antiferromagnetic cobalt oxide was formed. The EB field H_E is obtained from $H_E = |H_{c(+)} + H_{c(-)}|/2$, where, $H_{c(+)}$ and $H_{c(-)}$ are the coercive fields determined on the positive and negative field sweeping directions. At 20 K the FC curve exhibits a hysteresis loop shift H_E of 24 mT and a coercivity $H_{c(+)}$ of 3 mT. From FC hysteresis loops measured between 20 and 300 K, the values for $H_{c(+)}$ and H_E were extracted and plotted as a function of the temperature [Fig. 4(b)]. It is found that H_E strongly increases when measuring below the EB blocking temperature of $T_b \sim 100$ K. On the other hand, $H_{c(+)}$ first increases when reducing the temperature, which can be attributed to thermal fluctuations, but drops as H_E increases.

The latter observation indicates that the anisotropy causing $H_{c(+)}$ is aligned in a different direction compared to the magnetic field applied during FC (see Fig. 4, inset). The drop in $H_{c(+)}$ can be explained when considering the different thermal expansion coefficients α for Co and Si ($\alpha_{\text{Co}}=13 \times 10^{-6} \text{ K}^{-1}$ and $\alpha_{\text{Si}}=3 \times 10^{-6} \text{ K}^{-1}$ at room temperature)¹⁷ and adapting the model from Ref. 3. In the present case the tube length is considered to be constrained by the substrate whereas its diameter is free. Thus, when cooling from 300 to 20 K ($\Delta T=-280$ K) and using the elastic modulus for Co ($E_{\text{Co}}=204$ GPa at room temperature)¹⁸ the stress σ_0 amounts to ~ 570 MPa, with

$$\sigma_0 = E_{\text{Co}} \Delta T (\alpha_{\text{Si}} - \alpha_{\text{Co}}). \quad (2)$$

This changes stress along the tube axis from compressive ($\sigma_0 < 0$) into tensile stress ($\sigma_0 > 0$). As a consequence magnetic anisotropy is reversed, observable from the change in slope in Fig. 4(a).

In conclusion, the combination of strain engineering, lithography, and deposition techniques is an elegant approach to create well-defined arrays of magnetic microtubes. Our results provide insight into the magnetic switching behavior of rolled-up Au/Co/Au tubes in comparison to the initially flat magnetic films. The EB effect was observed at low temperatures. The tubes are of fundamental interest as well as importance for several applications^{6,7} and represent a class of integrative structures, which can be easily scaled in size by tuning the preparation parameters.

The authors acknowledge E. Coric for preparation of the TEM lamella. We thank B. Rellinghaus for the access to the FEI Tecnai 20 and D. J. Thurmer for manuscript reading.

¹T. Eimüller, T. Kato, T. Mizuno, S. Tsunashima, C. Quitmann, T. Ramsvik, S. Iwata, and G. Schatz, *Appl. Phys. Lett.* **85**, 2310 (2004).

²J. Rothman, M. Kläui, L. Lopez-Diaz, C. A. F. Vaz, A. Bleloch, J. A. C. Bland, Z. Cui, and R. Speaks, *Phys. Rev. Lett.* **86**, 1098 (2001).

³A. Kumar, S. Fähler, H. Schlröb, K. Leistner, and L. Schultz, *Phys. Rev. B* **73**, 064421 (2006).

⁴K. Nielsch, F. J. Castañó, C. A. Ross, and R. Krishan, *J. Appl. Phys.* **98**, 034318 (2005).

⁵C. Deneke, J. Schumann, R. Engelhard, J. Thomas, W. Sigle, U. Zschieschang, H. Klauk, A. Chuvilin, and O. G. Schmidt, *Phys. Status Solidi C* **5**, 2704 (2008).

⁶Y. F. Mei, G. Huang, A. S. Solovev, E. Bermúdez Ureña, I. Mönch, F. Die, T. Reindl, R. K. Y. Fu, P. K. Chu, and O. G. Schmidt, *Adv. Mater. (Weinheim, Ger.)* **20**, 4085 (2008).

⁷O. G. Schmidt and K. Eberl, *Nature (London)* **410**, 168 (2001).

⁸V. Y. Prinz, V. A. Seleznev, A. K. Gutakovskiy, A. V. Chehovskiy, V. V. Preobrazhenskii, M. A. Putyato, and T. A. Gavrilova, *Physica E (Amsterdam)* **6**, 828 (2000).

⁹A. Solovev, Y. F. Mei, E. Bermúdez Ureña, G. Huang, and O. G. Schmidt, "Catalytic microtubular jet engines self-propelled by accumulated gas bubbles," Small (in press).

¹⁰E. Bermúdez Ureña, Y. F. Mei, E. Coric, D. Makarov, M. Albrecht, and O. G. Schmidt, *J. Phys. D* **42**, 055001 (2009).

¹¹M. M. Hawkey and M. J. Brett, *J. Vac. Sci. Technol. A* **25**, 1317 (2007).

¹²C. Deneke, C. Müller, N. Y. Jin-Phillipp, and O. G. Schmidt, *Semicond. Sci. Technol.* **17**, 1278 (2002).

¹³G. P. Nikishkov, I. Khmyrova, and V. Ryzhii, *Nanotechnology* **14**, 820 (2003).

¹⁴A. Hubert and R. Schäfer, *Magnetic Domains: The Analysis of Magnetic Microstructures* (Springer, Berlin, 1998), p. 138.

¹⁵D. R. Lide, *CRC Handbook of Chemistry and Physics* (CRC, Boca Raton, 2008).

¹⁶J. Nogués and I. K. Schuller, *J. Magn. Magn. Mater.* **192**, 203 (1999).

¹⁷K. Schäfer and G. Beggerow, *Landolt Börnstein: Mechanische-Thermische Zustandsgrößen, Teil 1* (Springer, Berlin, 1971).

¹⁸W. Martienssen and H. Warlimont, *Handbook of Condensed Matter and Materials Data* (Springer, Heidelberg, 2005).